BEAM OPTICS FOR THE CEBAF FEL PROPOSAL*

D. V. Neuffer, D. Douglas, J. J. Bisognano
Continuous Electron Beam Accelerator Facility
12000 Jefferson Avenue, Newport News, VA 23606 USA

Abstract

Beam from the 45 MeV CEBAF injector linac can be used to drive a high-power infrared (IR) free electron laser (FEL), while the 400 MeV north linac beam can drive an ultraviolet (UV) FEL. The FELs require separation of high-intensity FEL driver bunches from the CEBAF nuclear physics beams into transport sections containing wigglers within optical cavities with appropriate matching. The FEL systems must fit within the CEBAF accelerator tunnel. Optical solutions for both the IR and UV FEL beam transports are described and discussed.

Introduction

The CEBAF superconducting linac will have unique capabilities for the acceleration of high-intensity electron beams. This capability can be applied to obtain beams suitable for driving infrared and ultraviolet free electron lasers. The IR FEL would use $\sim$ 50 MeV beam from the CEBAF injector, while the UV FEL would use $\sim$ 400 MeV beam from the CEBAF north linac. The FEL operation is being designed to accommodate simultaneous, undegraded nuclear physics operation [1,2].

FEL operation requires the addition of a high-peak current injector to provide FEL driver bunches and the addition of beam transport lines to separate the FEL driver bunches from the nuclear physics bunches and transport the beam into the FEL wigglers with betatron and dispersion matching. The FEL injector is described in [3,4]. In this paper we describe the IR and UV FEL beam transport lines and discuss their optical properties.

Beam Transport to the IR FEL

The IR FEL transport line must separate the FEL beam bunches from the nuclear physics (NP) beam at the end of the injector linac, with the NP beam continuing to the north linac, while the FEL beam is diverted into the IR wiggler. Figure 1 displays the proposed design. In this design we have chosen to obtain beam separation by accelerating the FEL and NP beams to different energies and using dipoles to separate the beams in a three-bend chicane.

Because of their large space-charge forces, it is desirable to accelerate the FEL bunches immediately to higher energy in the preinjector [2,3], where the two beams are initially combined. Thus the FEL bunches enter the injector linac at 10 MeV, while the NP bunches are at 5 MeV. For IR FEL operation this energy difference is maintained to the end of the injector linac where the FEL and NP beams are 50 and 45 MeV, respectively.

*Supported by the Commonwealth of Virginia

At that point (see Fig. 1), a 0.033 T-m bending magnet displaces both beams from a linear transport, with the FEL beam bent at 11.5° and the NP beam bent at 12.8°. At 1.2 m downstream the beams are separated by 2.5 cm, which is sufficient for a septum dipole which bends the FEL beam back by -23° toward the opposite side of the injector line. (The NP beam continues undeflected for another 0.5 m, where a -25.6° bend returns it toward the north linac injection line.) A 4 m transport containing three quads for dispersion correction carries the FEL beam to a third dipole, where the FEL beam is bent back 11.5° toward the wiggler. A 3.5 m transport containing four quads matches the beam into the wiggler, which is in the center of the 20 m optical cavity. After this last section, the FEL transport is parallel to the NP transport, displaced horizontally by 0.43 m. Following the wiggler, the FEL beam is diverted by a bending magnet into a beam dump.

The optical matching conditions are requirements of zero dispersion and betatron functions matched to the wiggler vertical focusing ($\beta^* = \sqrt{2}\ B\rho/B_{\rm rms} = 0.5$ m at $B_{\rm rms} = 0.45$ T). Betatron functions for such a solution are shown in Figure 2. Note that dispersion suppression requires relatively strong focusing of the beam in the interdipole transport with relatively large betatron oscillations. These matching conditions are somewhat stronger than the minimum necessary for FEL operation; FEL operation simply requires that the beam be smaller than the optical mode size W_0, given by $W_0 = (\lambda L_R/\pi)^{1/2}$, where λ is the light wavelength and L_R is the Rayleigh range. Typically W_0 is about 1.7 mm. At expected CEBAF beam properties ($\epsilon_N = 15\pi$ mm-mrad, $\delta p/p < 0.001$), optical constraints of $\beta^* < 10$ m, $\eta < 1$ m would be adequate.

Since dispersion correction most seriously constrains the matching, an alternative transport without the interdipole quads has also been developed. Without dispersion suppression, a betatron match is more easily found by simply using the final four quads. Focusing to small beam size ($\beta^* = 1$ m) also naturally reduces dispersion; the unmatched dispersion remains small ($\eta < 0.15$ m) throughout the wiggler. Dispersion matching is only necessary to avoid emittance dilution from wiggler radiation; that is of critical importance if the FEL beam is to be returned to the north linac to drive the UV FEL (a future option). However, since initially the FEL beam will not be reused, initial operation can use the simpler unmatched-η solution.

Beam Transport for the UV FEL

The transport to the UV FEL presents more difficult challenges because of the higher beam energy, more stringent phase-space matching constraints and a relatively restricted geometry. The transport must separate the FEL bunches from the NP bunch trains, provide longitudinal phase compression of the FEL bunch with a 6-D phase space match into the wiggler, and fit within the east end of the north linac tunnel. This last constraint implies a combined horizontal and vertical translation of the beam from the north linac transport line (outside lower corner of the tunnel) to the UV wiggler transport line (inside upper corner), which is placed to avoid interference with NP operation. A horizontal translation of 2.5 m and a vertical displacement of 1.75 m are required. Our proposed solution contains an innovative use of a solenoid (or skew-quad) phase-space rotator between the vertical and the horizontal beam translations; the rotation is designed to provide an isochronous 2-D dispersion cancellation.

As in the IR FEL, beam separation is obtained using energy separation. The UV FEL bunches are phased 25° off-crest, and arrive at the end of the north linac at 400 MeV, 10% lower energy than the first-turn NP bunches. The off-crest operation also places an energy tilt in the FEL bunches which is used to obtain compression.

Optical matching requirements are stricter for the UV FEL. The matched vertical β^* is $\sim$ 4 m (for 400 MeV beam, 0.45 T wiggler), which would give a beam size of $r_b \approx 0.3$ mm. However, the optical mode size is also $W_0 \approx 0.3$ mm (for $\lambda = 200$ nm, $L_R = 1.5$ m). For enhanced gain it is desirable to focus the beam to a smaller spot than the optical mode; $r_b = 0.15$ mm or $\beta^* = 1.0$ m is used. Accurate dispersion suppression is also required. The UV FEL beam has an enlarged $\delta p/p(\pm 0.004$ full-width); keeping that large momentum width within the optical mode sets a strict constraint on residual uncorrected dispersion ($|\eta| <\sim 0.05$ m).

Relatively stringent transport specifications have led to a modular, achromatic, and nearly isochronous beamline design. A layout of the system is shown in Figure 3. The FEL beam is separated from all NP beams by the common vertical dipole at the beginning of the east spreader. Vertical and then horizontal translations are followed by modules for bunch compression and matching into the wiggler. We now describe these in order.

After the common spreader dipole, the FEL beam (at 10% lower energy) is offset vertically from the nearest NP beam by over 10 cm at the first dipole of the NP recirculation line. This is adequate for insertion of a quad doublet to control FEL betatron sizes. The FEL beam is then bent back parallel to the linac axis, displaced vertically by 2 m.

To avoid the NP east arc while remaining in the tunnel, a horizontal translation is required. To avoid the complication of two-dimensional dispersion matching and to correct simultaneously the path-length dependence on momentum, a phase-space rotator is introduced to transform the (negative) vertical dispersion at the end of the vertical translation into a (positive) horizontal dispersion at the beginning of horizontal translation. The phase-space rotator consists of a single quadrupole followed by a solenoid. The quadrupole and the solenoid transform the vertical angular divergence into a horizontal dispersion with zero slope. The required solenoid strength is given by the condition: $\int B dl = \pi(B\rho)$. For 400 MeV beam, this requires a field integral of 42 kG-m. A phase-space rotator based on skew quadrupoles has also been designed but is operationally more complex and appears less cost-effective. The horizontal translation is generated using a dipole geometry identical to the vertical, and a quadrupole triplet is introduced for dispersion suppression; the resulting combined horizontal/vertical translation is achromatic and nearly isochronous.

Following the horizontal translation, a quad doublet is introduced. After the doublet, a bunch compression module based on a symmetric two-doublet insertion with an embedded horizontal three-dipole chicane provides an achromatic variation of path length with momentum without modification of betatron functions.

A pair of quad doublets then provides matching to the wiggler across a final dispersion-suppressed vertical transverse translation. This final translation onto the axis of the wiggler and optical cavity is a 0.5 m offset provided to ensure the optical beam clears all beam transport equipment. The final matching telescope can be tuned to provide a range of matching conditions. We have investigated the case of a 3 m, 50 period wiggler. Figure 4 presents rms beam spot sizes though the system for a quasi-isochronous (no compression) case with final match to upright ellipses with $\beta^{\rm wiggler} = 1$ m at the center of the wiggler, in both planes. Following the wiggler, spent beam is transported to a beam dump in the north linac tunnel stub.

The strong bending and focusing of the beam in this transport channel, coupled with the desired large momentum acceptance and strict transport requirements, lead to a requirement for chromatic correction. Suppression of chromatic aberrations to acceptable levels is performed using a pair of sextupoles, one normal and one skew, immediately upstream of the phase-space rotator. The skew sextupole acts on η_y and corrects the final T_{166}, where T_{166} is the second-order transport element $\partial x/\partial(\frac{\Delta p}{p})^2$. The normal sextupole introduces some horizontal/vertical coupling, which is compensated by the residual coupling due to the rotator yielding a correction of T_{366}. Correcting these two aberrations also reduces T_{566} to acceptable levels. Variations at wiggler center of central orbit position, path length, and spot sizes, over the full momentum range, with and without chromatic correction, have been calculated with $\beta_x^{\rm wiggler} = \beta_y^{\rm wiggler} = 1$ m at wiggler center. The results are consistent with desired criteria.

Acknowledgments

We gratefully acknowledge assistance from C. Rode, C. Leemann, and G. Neil.

References

[1] G. R. Neil *et al.*, NIM A318, p. 212 (1992).
[2] Proposal: High-Power UV and IR Free Electron Lasers Using the CEBAF Superconducting Accelerator, May 1991 (unpublished).
[3] P. Liger *et al.*, these proceedings (1992).
[4] P. Liger *et al.*, NIM A318, p. 290 (1992).

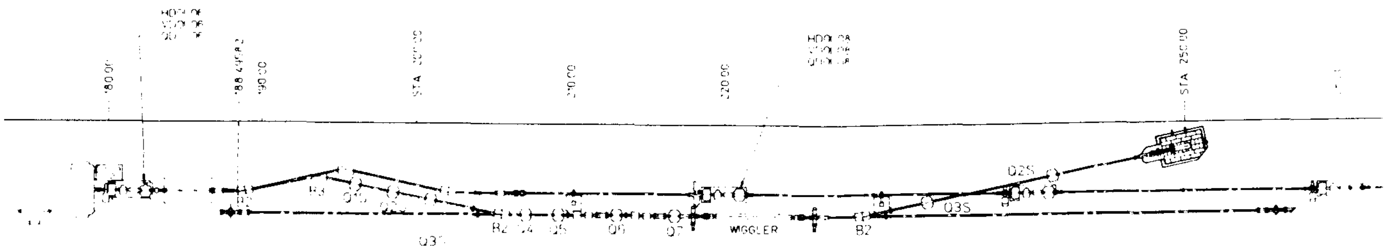

Figure 1. Beam transport for the IR FEL, with the injector linac transport.

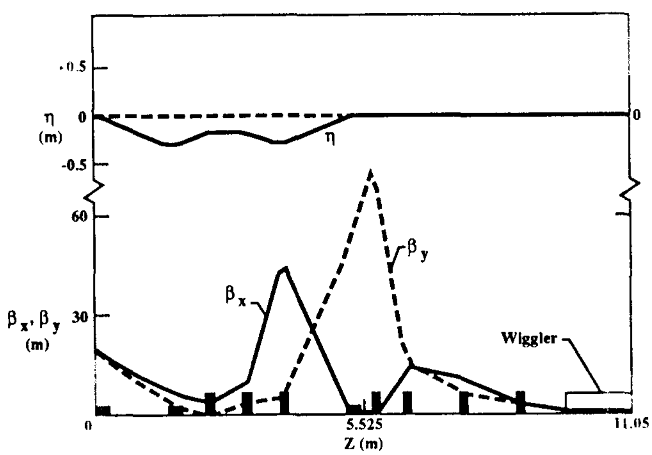

Figure 2. Betatron functions (β_x, β_y, η) through the IR FEL beam transport. The 1.5 m IR wiggler is at the end of the transport line.

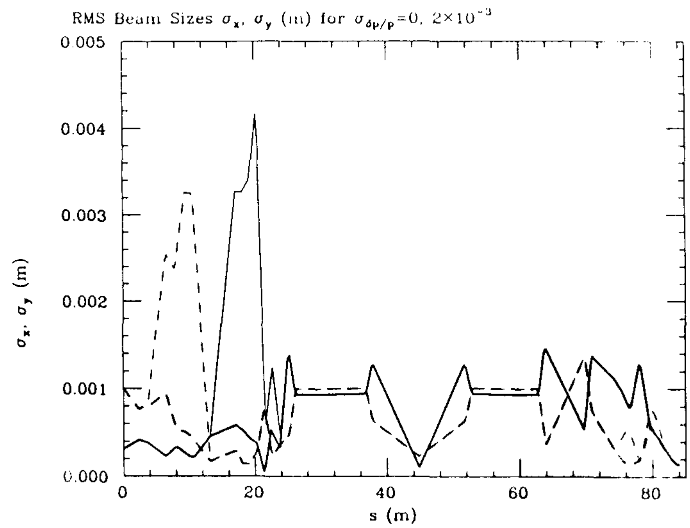

Figure 4. Horizontal and vertical rms spot sizes (σ matrix elements σ_x and σ_y) through transport system, from linac to wiggler center. Uncoupled unnormalized initial emittances $\epsilon_x = \epsilon_y = 2 \times 10^{-8}$ m-rad were assumed. Solid lines indicate the horizontal, and dashed lines the vertical, spot size; bold lines indicate beam size with $\sigma_{\delta p/p} = 0$ (dispersive effects neglected); light lines indicate beam size with the anticipated $\sigma_{\delta p/p} = 2 \times 10^{-3}$.

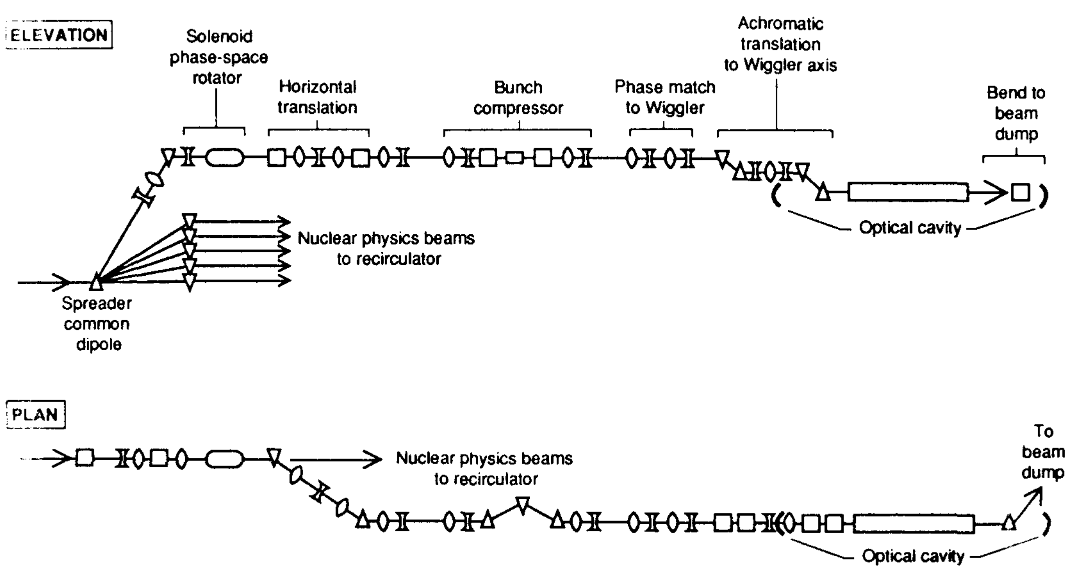

Figure 3. Schematic view of the beam transport for the UV FEL.